Science Advances

▲AAAS

Supplementary Materials for

EGFR is a master switch between immunosuppressive and immunoactive tumor microenvironment in inflammatory breast cancer

Xiaoping Wang *et al.*

Corresponding author: Naoto T. Ueno, nueno@cc.hawaii.edu; Xiaoping Wang, xiwang@mdanderson.org

This PDF file includes:

Supplementary Text
Figs. S1 to S5
Tables S1 to S4
References

Supplementary Text

Supplementary methods

Materials and reagents

The following reagents were used: Matrigel Matrix (BD Biosciences), IgG2 and InVivoMab anti-human PD-L1 antibody (clone 29E.2A3) (Bio X Cell); panitumumab (MD Anderson pharmacy); Tumor Dissociation Kit (Miltenyi Biotec); RBC lysis buffer and fluorochrome-coupled antibodies against APC/Cy7-mouse CD45, FITC-human CD45, APC-human CD45, PE/Cy7-human CD3, Alexa Fluor488-human CD8, APC-human CD4, PE-human CD127, and Pacific Blue-human CD25 (BioLegend); LIVE/Dead Fixable Aqua Dead Cell stain kit, ProLong Diamond Antifade Mountant, citrate plus solution, formaldehyde, Lipofectamine RNAiMAX, Pierce IP Lysis Buffer, and RNase (Thermo Fisher Scientific); recombinant human protein EGF and human ELISA kits (CCL2 DY279-05, CCL20 DY360-05, CXCL5 DX000, and IL8 DY208) (R&D Systems); M-CSF, IL-4, IL-13, CCL4, CCL5, CXCL9, CXCL10, IL-8, CCL2, CXCL5, and CCL20 (PeproTech); MG-132 (Sigma-Aldrich); Ficoll-Paque PLUS and nProtein A/Protein G Sepharose 4 Fast Flow beads mix (GE Healthcare); Opal Polaris 480 or 780 reagent pack and Opal Polaris 7 color automation IHC detection kit (Akoya Biosciences); human cytokine antibody array and chromatin extraction kit (Abcam); protease inhibitor and phosphatase inhibitor cocktails (Bimake, B14002 and B15001); RNeasy Mini Kit (Qiagen); SuperScript II Reverse Transcriptase Kit, Dynabeads Untouched Human CD8 T Cells kit, Dynabeads Regulatory CD4$^+$/CD25$^+$ T Cell kit, and PureLink PCR purification kit (Invitrogen); Power SYBR Green PCR Master Mix (Applied Biosystems); ImmunoCult Human CD3/CD28 T Cell Activator and IL-2 (STEMCELL Technologies); CellTiter-Blue (Promega); LiCl Immune Complex Wash Buffer (Millipore Sigma); and proteinase K (ApexBio).

The following primary antibodies were used for Western blot: anti-phospho-EGFR (Tyr1086) (Cell Signaling, #2220), EGFR (Santa Cruz Biotechnology, sc-03-G), EGR1 (Cell Signaling, #4154S), pERK (Cell Signaling, #4370), ERK (Cell Signaling, #4695), pAKT (Cell Signaling, #4060), AKT (Cell Signaling, #9272), α-Tubulin (Millipore Sigma, MABT522), and β-Actin (Millipore Sigma, MAB1522). The following primary antibodies were used for immunohistochemical (IHC) staining: anti-phospho-human EGFR (Abcam, ab40815), anti-human EGR1 (Abcam, ab194357), and anti-human Ki67 (Cell Signaling, #9027S).

The following primary antibodies were used for multiplexed immunofluorescence staining: anti-human CD8 antibody (Abcam, ab4055, 1:50 dilution with Blocking/Ab Diluent), anti-human CD68 antibody (Millipore Sigma, SAB5500070, 1:100 dilution), anti-human CD3 antibody (Abcam, ab16669, 1:200 dilution), anti-human CD163 antibody (Cell Marque, AC 0316A, 1:100 dilution), anti-human FoxP3 antibody (Abcam, ab20034, 1:100 dilution), anti-human CK7 antibody (Agilent Dako, M7018, 1:200 dilution), and anti-human Granzyme B antibody (Leica Bond, Granzyme-b, no dilution).

Multiplexed immunofluorescence staining and imaging

The expression of human CD3, CD8, CD68, CD163, FoxP3, and cytokeratin 7 (CK7) in SUM149- or BCX010-hu-NSG-SGM3 tissues or IBC patient tissues was analyzed using the Opal Polaris 7 color automation IHC detection kit following the manufacturer's instructions. Briefly, 5-µm FFPE slides were deparaffinized before antigen retrieval in citrate plus solution heated at 95°C for 15 min using the BioGenex EZ-Retriever microwave system. After treatment with 0.6% hydrogen peroxide for 5 min to block endogenous peroxidase activity and with 3% BSA for 1 h to block nonspecific binding, slides were incubated with primary anti-human CD8 antibody for 1 h at room temperature (RT). Then slides were incubated with secondary HRP-

conjugated antibody for 10 min at RT. Opal signal was amplified by incubation with Opal TSA Fluorophore 620 for 10 min at RT. Then slides were subjected to antigen retrieval as described above to remove bound antibodies before sequential staining with the following antibodies: anti-human CD68 (TSA 520), CD3 (TSA 480), CD8 (TSA 620), CD163 (TSA 690), FOXP3 (TSA 570), and CK7 (Opal Polaris 780) antibodies. After completion of all 6 sequential reactions, slides were counterstained with DAPI for 5 min at RT and mounted with ProLong Diamond Antifade Mountant. Multiplex stained slides were imaged using Vectra 3.0 (PerkinElmer) at 20× magnification. inForm Tissue Analysis Software version 3.0 (Akoya) was used to analyze images, including cell segmentation, phenotyping, and cell quantitation. Cells were phenotyped as cancer cells (CK7$^+$), cytotoxic T cells (CD3$^+$CD8$^+$), Tregs (CD3$^+$FOXP3$^+$), or M2 macrophages (CD68$^+$CD163$^+$). The average number of different cell types was quantitated on 5 high-power fields. A similar method was used to stain another 2 panels of markers on SUM149-hu-NSG-SGM3 mouse tissues. Panel 1 included CD3, CD8, CD45RO, FOXP3, Granzyme B, and AE1/3 (broad-spectrum cytokeratin), and panel 2 included CD3, CD8, CD68, PD-L1, PD-1, and AE1/3.

In vitro **immune cell migration assay**

To obtain peripheral blood mononuclear cells (PBMCs), healthy donors' buffy coats were purchased from Gulf Coast Regional Blood Center. PBMCs were isolated from the buffy coats by density gradient centrifugation with Ficoll-Paque PLUS, then seeded in cell culture plates with RPMI-1640 medium supplemented with 10% FBS (10% FBS/RPMI). Floating cells were collected after 3 h and cultured in a cell culture flask at a cell density of 1×10^6 cells/ml with 10% FBS/RPMI, 25 µg/ml ImmunoCult Human CD3/CD28 T Cell Activator, and 10 ng/ml human recombinant IL-2 for 3 days and expanded by addition of fresh 10% FBS/RPMI and

human recombinant IL-2 every 2-3 days. CD8$^+$ T cells and Tregs were purified by using the Dynabeads Untouched Human CD8 T Cells kit and Dynabeads Regulatory CD4$^+$/CD25$^+$ T Cell kit. In parallel, attached cells were cultured for 6 days with 10% FBS/RPMI supplemented with 10 ng/ml human M-CSF to induce differentiation into macrophages followed by stimulation with 20 ng/ml IL-4 and IL-13 for 2 days to induce polarization into M2 macrophages. For CD8$^+$ T cell migration assay, 1×10^4 CD8$^+$ T cells suspended in serum-free RPMI-1640 medium were seeded on the top chamber of a 96-well migration plate with 8-μm pores (Sartorius), and 10% FBS/RPMI, 10% FBS/RPMI supplemented with 100 ng/ml recombinant human CCL4, CCL5, CXCL9, and CXCL10 individually or in combination, or CCL20 were added to the bottom chamber. For Treg or M2 macrophage migration assay, 2×10^3 Tregs or 1×10^4 M2 macrophages suspended in serum-free RPMI-1640 medium were seeded on the top chamber of a 96-well migration plate, and 10% FBS/RPMI or 10% FBS/RPMI supplemented with 100 ng/ml recombinant human CCL2, CCL20, CXCL5, or IL-8 individually or in combination were added to the bottom chamber. Cells were incubated at 37°C in a CO$_2$ incubator for 48 h, and then cell migration was quantified by CellTiter-Blue. For co-culture migration assay, 1×10^4 SUM149 shCtrl cells or EGFR knockdown clones shEGFR-4 or shEGFR-5 were seeded in the bottom chamber with 10% FBS/RPMI and incubated for 4 h. Then the bottom of the top chamber was coated with growth factor reduced Matrigel, and 2×10^3 Tregs or 1×10^4 M2 macrophages suspended in serum-free RPMI-1640 medium were seeded into the top chamber. After incubation for 48 h, the migrated cells were detached from the bottom side of the top chamber using dissociation solution supplied with the Cultrex Cell Migration Assay kit (R&D Systems) and quantified by CellTiter-Blue. Relative migration was calculated as fold change compared to 10% FBS.

RNA isolation and quantitative RT-PCR

Primer sequences for quantitative RT-PCR were as follows: *IFNγ* forward, 5'-ATGAACGCTACACACTGCATC-3'; *IFNγ* reverse, 5'-CCATCCTTTTGCCAGTTCCTC-3'; *CCL4* forward, 5'-CTGTGCTGATCCCAGTGAATC-3'; *CCL4* reverse, 5'-TCAGTTCAGTTCCAGGTCATACA-3'; *CCL5* forward, 5'-CCAGCAGTCGTCTTTGTCAC-3'; *CCL5* reverse, 5'-CTCTGGGTTGGCACACACTT-3'; *CXCL9* forward, 5'-CCAGTAGTGAGAAAGGGTCGC-3' ; *CXCL9* reverse, 5'-AGGGCTTGGGGCAAATTGTT-3' ; *CXCL10* forward, 5'-GTGGCATTCAAGGAGTACCTC-3' ; *CXCL10* reverse, 5'-TGATGGCCTTCGATTCTGGATT-3' ; *CCL2* forward, 5'-TTAAAAACCTGGATCGGAACCAA-3'; *CCL2* reverse, 5'-GCATTAGCTTCAGATTTACGGGT-3'; *CCL20* forward, 5'-TGTGTGCGCAAATCCAAAACA-3' ; *CCL20* reverse, 5'-GAAACCTCCAACCCCAGCAA-3'; *CXCL5* forward, 5'-CAAGTTCCCTCCCCACTCAC-3'; *CXCL5* reverse, 5'-TGCTAAAAACCCGACAGGCA-3'; *IL-8* forward, 5'-TTTTGCCAAGGAGTGCTAAAGA-3'; *IL-8* reverse, 5'-AACCCTCTGCACCCAGTTTTC-3'; *EGR1* forward, 5'-TGAAACAGCAGTCCCAGTATTC-3'; *EGR1* reverse, 5'-GAGAGTACGGTCAAGCAGTATTT-3'; *GAPDH* forward, 5'-TGCACCACCAACTGCTTAGC -3'; *GAPDH* reverse, 5'- GGCATGGACTGTGGTCATGAG -3'; *RPL3* forward, 5'-AAAGAGGACCAAGAAGTTCATTAGG-3'; and *RPL3* reverse, 5'-CGCCAGTTCCGCTTGATTT-3'.

EGFR or EGR1 stable or transient knockdown in IBC cells

The sequences of shEGR1 clones were

CCGGCGACATCTGTGGAAGAAAGTTCTCGAGAACTTTCTTCCACAGATGTCGTTTTT

(shEGR1-B) and

CCGGCGGTTACTACCTCTTATCCATCTCGAGATGGATAAGAGGTAGTAACCGTTTTT

(shEGR1-C). Mission Non-Target shRNA Control Transduction Particles (SHC002V) were used

as a control. Stable control (shCtrl) and EGFR or EGR1 knockdown clones (shEGFR-4 and -5;

shEGR1-B and -C) were selected and maintained with puromycin (1 µg/ml). EGR1 expression in

BCX010 cells was transiently knocked down using 2 specific siRNAs (SASI_Hs01_00232227

and SASI_Hs01_00232228, Millipore Sigma).

Analysis of expression of chemokines in patients with IBC

We analyzed the mRNA expression data of 137 IBC and 252 non-IBC clinical samples (N =

389) collected within the World IBC Consortium (*22*). IBC was defined clinically according to

international consensus criteria (*71*). Collection criteria and sample characteristics have been

previously described (*22*). Briefly, all samples were pretreatment primary tumor samples from

patients with invasive breast adenocarcinoma treated at the Institut Paoli-Calmettes (Marseille,

France), the General Hospital Sint-Augustinus (Antwerp, Belgium), and MD Anderson Cancer

Center (Houston, USA). IBC samples were diagnostic biopsy specimens taken from

consecutively treated patients, clinically annotated, and with good-quality tumor RNA. Non-IBC

samples were either diagnostic biopsy specimens (advanced-stage disease) or surgical specimens

(early-stage disease). Each patient gave written informed consent, and institutional review boards

approved the study. The patients had been treated using the classical guidelines. Neoadjuvant

chemotherapy delivered to IBC patients was anthracycline-based, often including taxane, and

associated with trastuzumab in more than 50% of HER2-positive cases. Chemotherapy was

followed by mastectomy and axillary lymph node dissection for clinically non-progressive and

consenting patients, then radiotherapy. After radiotherapy, adjuvant hormone therapy was given

to patients with estrogen receptor (ER)-positive IBC and adjuvant trastuzumab was given to patients with *ERBB2* amplification. Survival of IBC patients was calculated from the date of diagnosis to the date of first distant metastatic relapse for metastasis-free survival and death from any cause for overall survival.

The gene expression profiles of samples had been generated using Affymetrix platforms in each institution for its samples (U133 Plus 2.0 human microarrays for the France and Belgium institutions and U133A human microarrays for the US institution) as previously described (*22*). Each dataset was briefly normalized using Robust Multichip Average in R using Bioconductor and associated packages (*72*). We then merged the 3 datasets by using COMBAT (empirical Bayes) (*73*) as a batch effects removal method, included in the inSilicoMerging R/Bioconductor package (*74*). When multiple probes mapped to the same GeneID, we retained the one with the highest variance. ER, progesterone receptor (PR), and ERBB2/HER2 statuses of samples were based on mRNA expression of the 205225_at (*ESR1*), 208305_at (*PGR*), and 216836_s_at (*ERBB2*) Affymetrix probe sets and defined as discrete values (positive/negative) using a 2-component Gaussian mixture distribution model (*75*). The molecular subtypes of tumors were defined as HR+/HER2- (ER- and/or PR-positive and HER2-negative), HER2+ (HER2-positive, regardless of ER and PR), and triple-negative (ER-, PR-, and HER2-negative).

Chromatin immunoprecipitation assay

IBC SUM149 cells (1×10^7) were fixed with formaldehyde at a final concentration of 0.75% for 10 min at RT and then incubated with 125 mM glycine 5 min at RT. After washing with cold PBS 2 times, cells were collected and snap-frozen in liquid nitrogen. DNA fragments were prepared using a chromatin extraction kit according to the manufacturer's instructions. DNA fragments were then diluted with Pierce IP Lysis Buffer, incubated with rabbit IgG or anti-EGR1

antibody overnight at 4°C, and then incubated with pre-washed nProtein A/Protein G Sepharose 4 Fast Flow beads mix for 3 h at 4°C. After centrifugation, pellets were washed with low-salt buffer (0.1% SDS, 1% TritonX-100, 2 mM EDTA, 20 mM Tris-HCL, 150 mM NaCl), high-salt buffer (0.1% SDS, 1% TritonX-100, 2 mM EDTA, 20 mM Tris-HCL pH 8.0, 500 mM NaCl), and LiCl Immune Complex Wash Buffer. DNA was then eluted with elution buffer (1% SDS, 100 mM NaHCO$_3$) followed by RNase and proteinase K treatment and purified using a PureLink PCR purification kit. Purified DNA was used as a template and was subjected to qRT-PCR for *CCL2*, *CCL20*, *CXCL5*, and *IL-8* genes. The primer sequences were as follows: *CCL2* forward, 5'-TGCCTTTGTCCAAGTCTGAAACCC-3'; *CCL2* reverse, 5'-TTGGCCGGCTCCCTGACAAT-3'; *CCL20* forward, 5'-TAAGAAACCATGCCCACACA-3'; *CCL20* reverse, 5'-GCAAGGCAGCCACTAAGAAC-3'; *CXCL5* forward, 5'-CCCCTGGGAAATAGATGACA-3'; *CXCL5* reverse, 5'-TGGAAGACTGGGAGCAGAGT-3'; *IL-8* forward, 5'- GGGCCATCAGTTGCAAATC-3'; *IL-8* reverse, 5'-GCTTGTGTGCTCTGCTGTCTC-3'; negative control forward, 5'-CTCCCAAATTGCTGGGATTA-3'; negative control reverse, 5'-ATTCCAGGCACCACAAAAAG-3'.

IHC staining

Tumor tissues from SUM149- or BCX010-hu-NSG-SGM3 mice treated with IgG2 or panitumumab were formalin-fixed and paraffin-embedded. The effect of panitumumab on the expression of pEGFR, EGR1, and Ki67 *in vivo* was evaluated by IHC staining as described previously (*76*). IHC staining was quantified by using Fiji (https://imagej.net) to calculate the proportion of DAB-stained tissue (% of total area) in at least 3 images.

Western blot analysis

SUM149 or BCX010 cells were treated with panitumumab at 20 µg/ml for different times. For EGF stimulation, SUM149 or BCX010 cells were serum-starved for 24 h and stimulated with EGF (20 ng/ml) for different times with or without panitumumab (20 µg/ml), erlotinib (1 µM), or MG-132 (5 µM) pretreatment. In addition, Western blot analysis was performed as described previously (*77*).
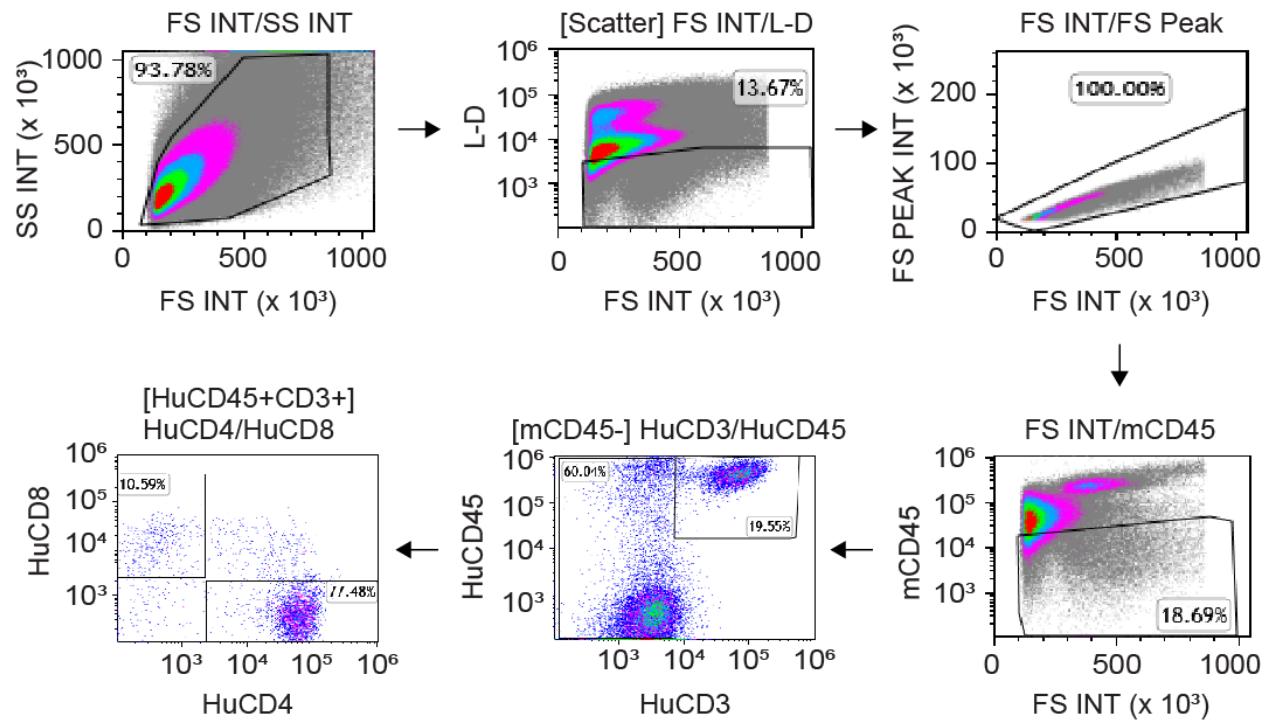
Fig. S1.

Fig. S1. Human immune cells in IBC humanized mouse model. The presence of human immune cells, including CD45^{+}, CD3^{+}, CD4^{+}, and CD8^{+} cells, in SUM149-hu-NSG-SGM3 tumor tissues by flow cytometry.
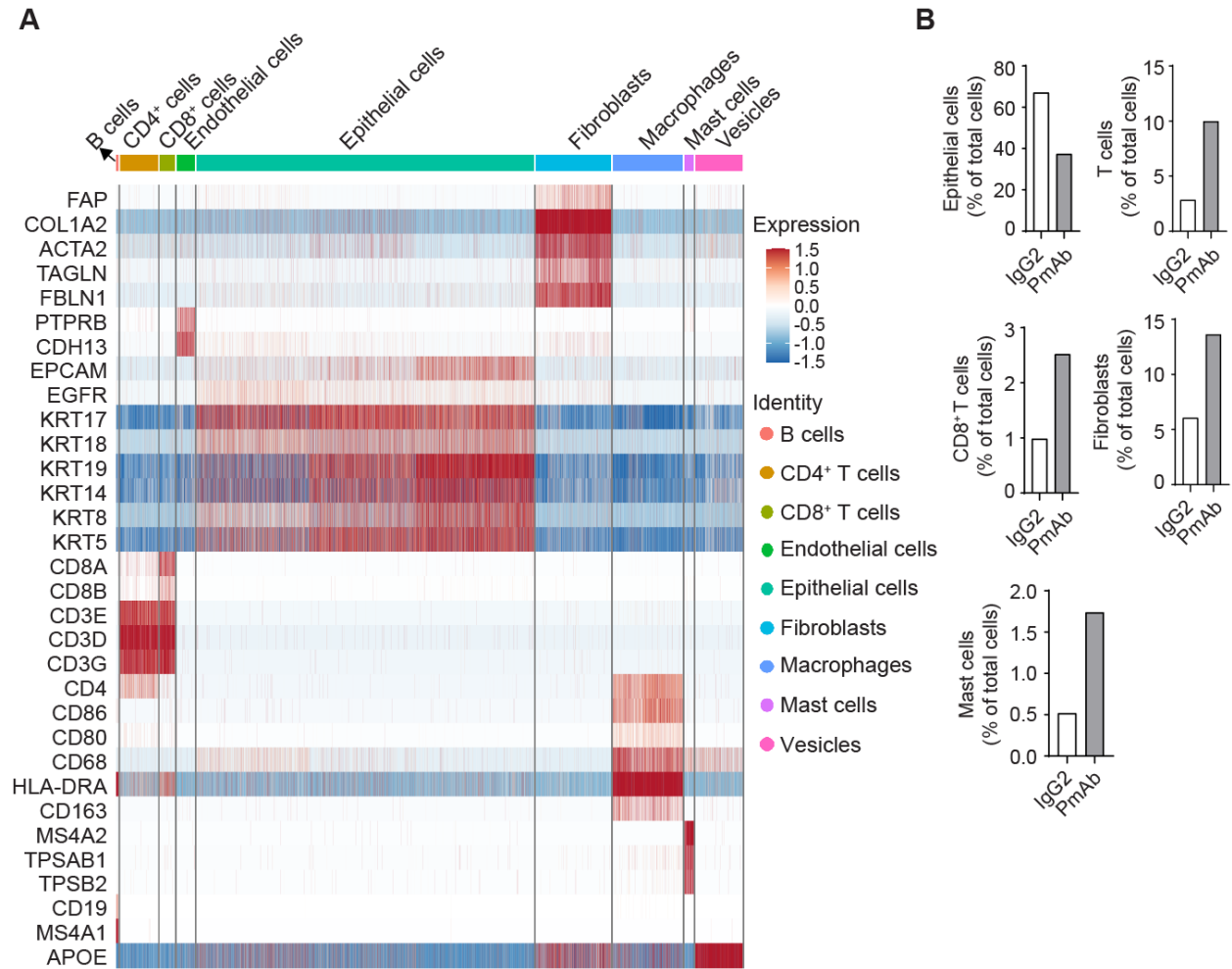
Fig. S2.

Fig. S2. scRNA-seq of SUM149-hu-NSG-SGM3 tumors treated with IgG2 and panitumumab. (**A**) Heat map of marker gene expression in each cell type used in the downstream analysis. (**B**) Populations of epithelial cells, T cells, CD8+ T cells, fibroblasts, and mast cells in IgG2- and panitumumab-treated SUM149-hu-NSG-SGM3 tumors as analyzed by scRNA-seq. PmAb: panitumumab.

Fig. S3.

A Epithelial cells

C Interferon_alpha_response
NES = 1.3532
FDR q = 0.06472
PmAb   IgG2

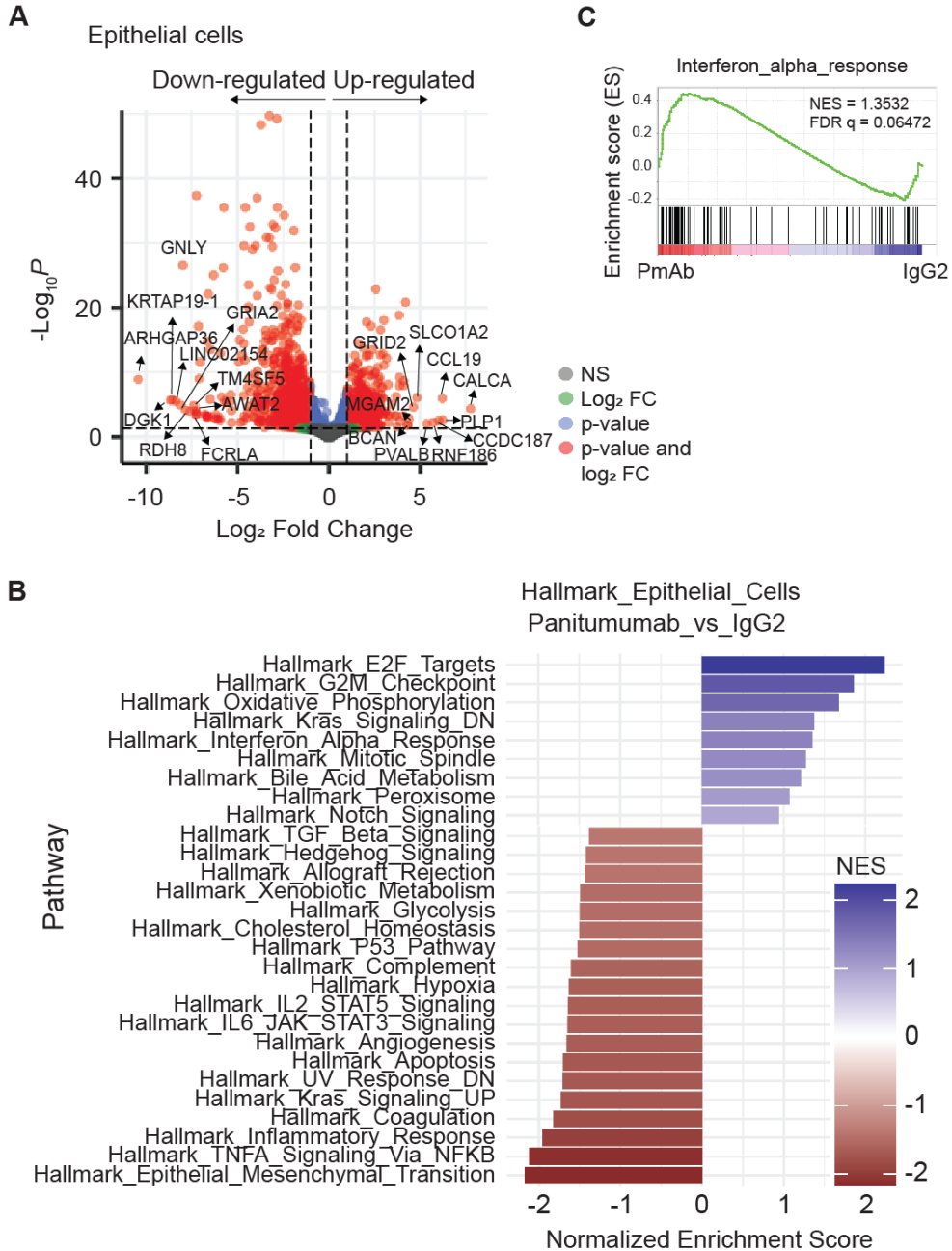**B** Hallmark_Epithelial_Cells
Panitumumab_vs_IgG2

Fig. S3. **Differential gene expression in epithelial cells from SUM149-hu-NSG-SGM3 mice treated with IgG2 and panitumumab.** (**A**) Volcano plot of significantly differentially expressed genes in epithelial cells after panitumumab treatment. Top 10 upregulated and

downregulated genes are labelled. (**B**) Gene set enrichment analysis of epithelial cells after

panitumumab treatment using Hallmark pathway database. (**C**) Enrichment of genes associated

with interferon-alpha response in panitumumab-treated SUM149 tumor in humanized mice. This

pathway has been shown to modulate innate and adaptive compartments to provide a pro-

inflammatory context suitable for dendritic cell antigen presentation, priming of T lymphocytes,

and increasing cytotoxic functions of NK cells (*29-31*). PmAb: panitumumab. FC: fold change.
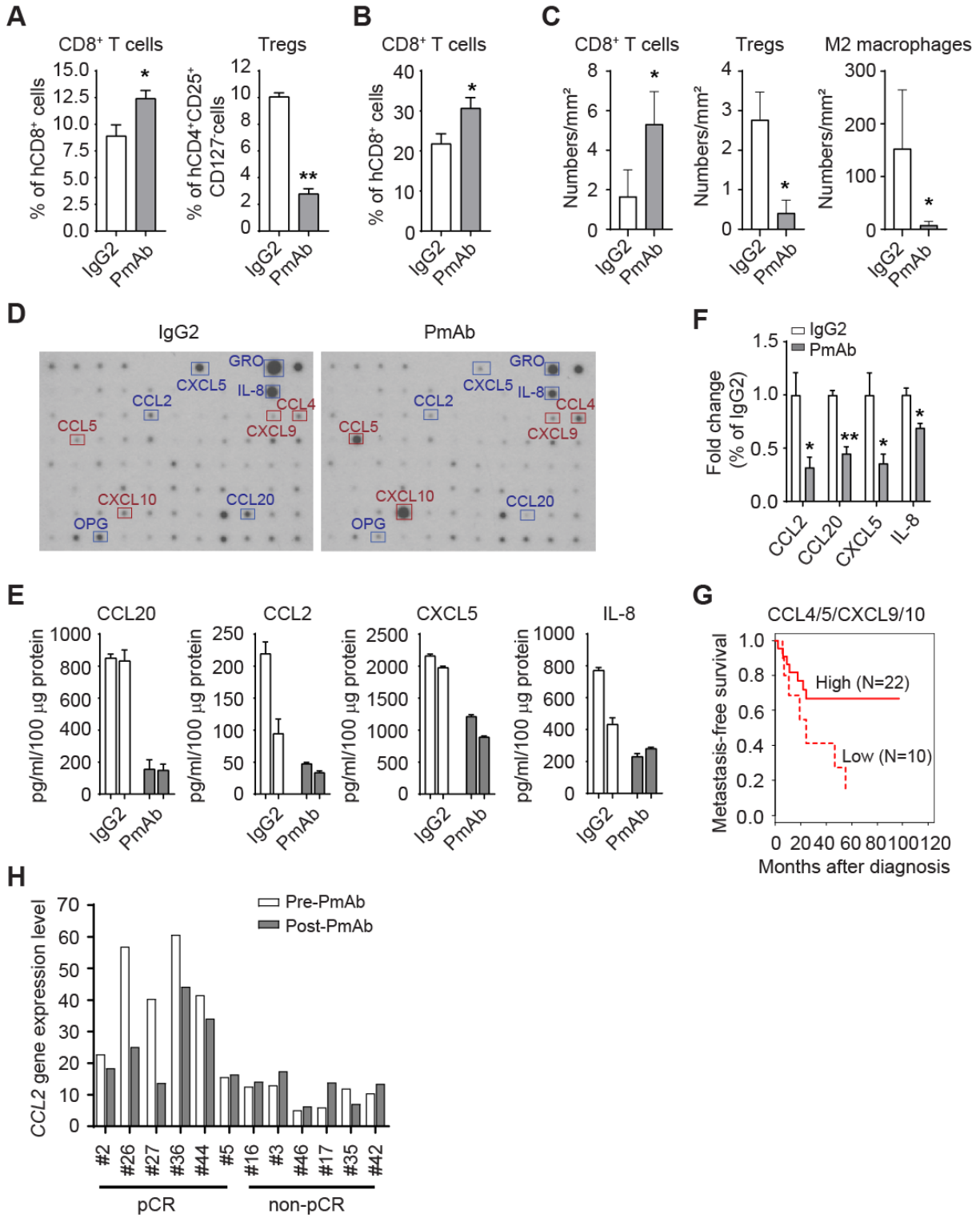
Fig. S4.

Fig. S4. Panitumumab treatment affects the immunosuppressive TME through regulating the expression of chemokines in IBC cells. (**A**) Flow cytometry analyses of CD8$^+$ T cells and Tregs in peripheral blood of SUM149-hu-NSG-SGM3 mice treated with IgG2 and panitumumab. * $P < 0.05$, ** $P < 0.01$. (**B**) Flow cytometry analyses of CD8$^+$ T cells in tissues of BCX010-hu-NSG-SGM3 mice treated with IgG2 and panitumumab. * $P < 0.05$. (**C**) CD8$^+$ T cells, Tregs, and M2 macrophages in tissues of BCX010-hu-NSG-SGM3 mice treated with IgG2 and panitumumab analyzed by multiplexed immunofluorescence staining. * $P < 0.05$. (**D**) Cytokine antibody array in tumors from humanized SUM149-hu-NSG-SGM3 mice treated with IgG2 and panitumumab. (**E**) CCL20, CCL2, CXCL5, and IL-8 protein in tumors from humanized SUM149-hu-NSG-SGM3 mice treated with IgG2 and panitumumab analyzed by ELISA. (**F**) *CCL2*, *CCL20*, *CXCL5*, and *IL-8* gene expression in tumors from humanized BCX010-hu-NSG-SGM3 mice treated with IgG2 and panitumumab analyzed by qRT-PCR. * $P < 0.05$, ** $P < 0.005$. (**G**) Kaplan-Meier metastasis-free survival (MFS) curves in patients with triple-negative IBC (TN-IBC) with high (N = 22) and low (N = 10) metagene scores of *CCL4, CCL5, CXCL9,* and *CXCL10* mRNA expression. The 5-year MFS rate was 67% in patients with high expression and 14% in those with low expression ($P = 3.09E-02$). (**H**) Correlation of changes in *CCL2* gene expression level after panitumumab treatment with status of pathologic complete response (pCR) to neoadjuvant chemotherapy combined with panitumumab in patients with IBC. pCR patients: *P* = 0.0625; non-pCR patients: *P* = 0.438. Data are summarized as mean ± SD in panels A-C and E-F. PmAb: panitumumab. Experiment in panel F was independently repeated 3 times with 3 replicates each time.
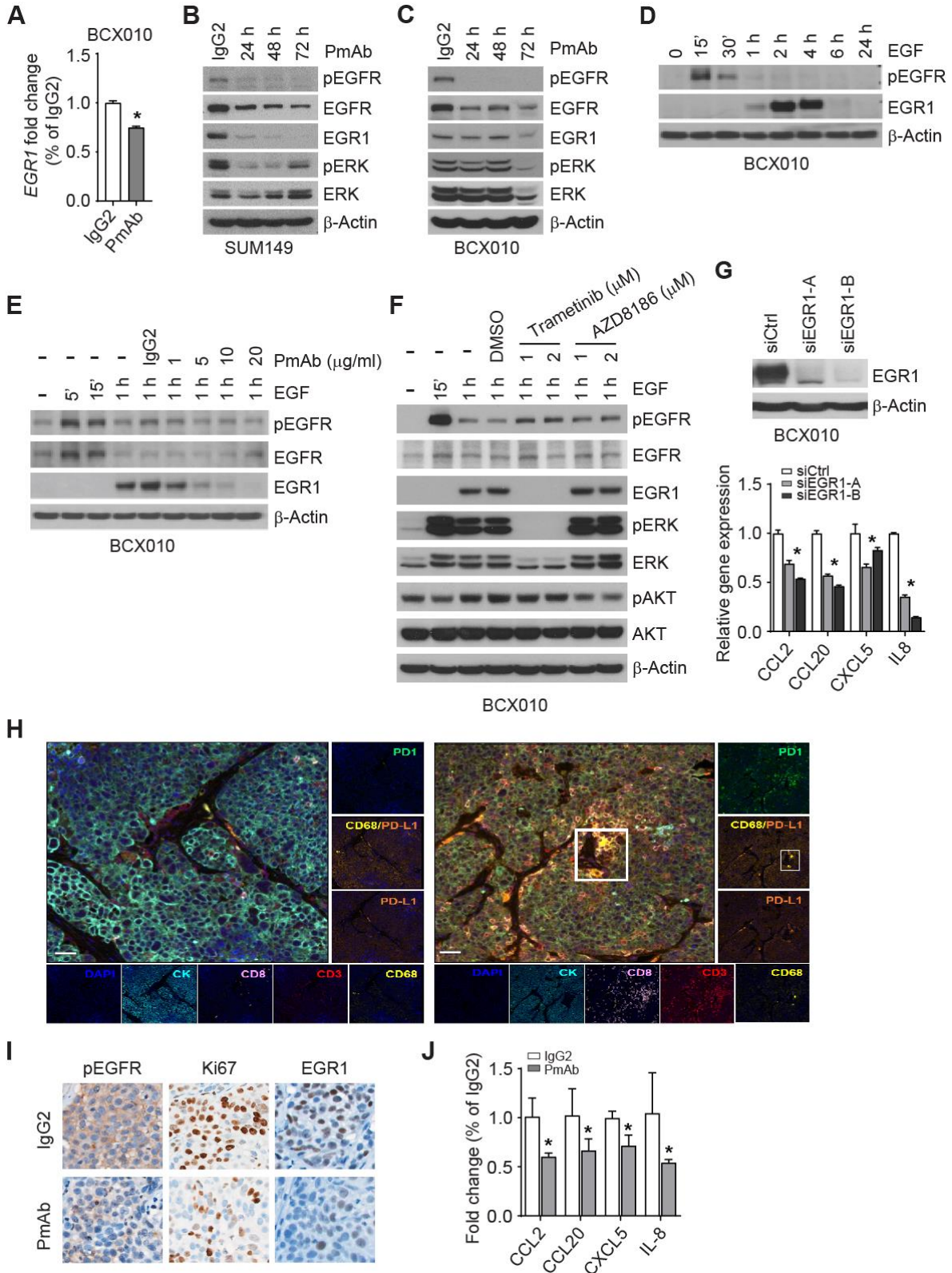
Fig. S5.

A BCX010

B SUM149

C BCX010

D BCX010

E BCX010

F BCX010

G BCX010

H

I

J

Fig. S5. EGFR pathway regulates the expression of CCL2, CCL20, CXCL5, and IL-8 through EGR1 in IBC. (**A**) Panitumumab treatment reduces the gene expression of *EGR1* in BCX010 cells by RT-PCR. * $P < 0.05$. (**B** and **C**) Panitumumab (20 µg/ml) treatment reduces the expression of EGR1 in SUM149 (**B**) and BCX010 cells (**C**). (**D**) EGF (20 ng/ml) stimulates the expression of EGR1 in BCX010 cells. (**E**) Pretreatment with panitumumab mitigates the upregulation of EGR1 by EGF stimulation in BCX010 cells. (**F**) Pretreatment with MEK inhibitor trametinib, but not PI3K inhibitor AZD8186, inhibits the upregulation of EGR1 by EGF stimulation in BCX010 cells. (**G**) EGR1 knockdown (top panel) reduces the expression of *CCL2*, *CCL20*, *CXCL5*, and *IL-8* genes in BCX010 cells (bottom panel). * $P < 0.01$. (**H**) Panitumumab-treated tissues have more CD68$^+$PD-L1$^+$ cells than IgG2-treated tissues in SUM149-hu-NSG-SGM3 mice as analyzed by multiplexed immunofluorescence staining. Scale bar: 50 µm. (**I**) IHC staining of pEGFR, Ki67, and EGR1 in tumor tissues from SUM149-hu-NSG-SGM3 mice treated with IgG2 and panitumumab of Fig. 5A. (**J**) Panitumumab treatment reduces the expression of *CCL2*, *CCL20*, *CXCL5*, and *IL-8* gene in tumor tissues from SUM149-hu-NSG-SGM3 treated with IgG2 and panitumumab of Fig. 5A. * $P < 0.05$. Data are summarized as mean ± SD in panels A, G, and I. PmAb: panitumumab. Experiments in panels A, G, and J were independently repeated 3 times with 3 replicates each time. Experiments in panels B-F were independently repeated 3 times.

Table S1. Gene set enrichment analysis showing the top 10 negatively enriched and 5 positively enriched pathways in panitumumab-treated compared to IgG2-treated SUM149-hu-NSG-SGM3 tumor cells.

Rank	Name	Size	ES	NES	Nominal P Value	FDR q Value	FWER P Value
Negative enrichment in panitumumab-treated tissue							
1	HALLMARK_EPITHELIAL_MESENCHYMAL_TRANSITION	197	-0.7509	-2.1700	0.0	0.0	0.0
2	HALLMARK_TNFα_SIGNALING_VIA_NFκB	198	-0.7419	-2.1188	0.0	0.0	0.0
3	HALLMARK_INFLAMMATORY_RESPONSE	193	-0.6831	-1.9586	0.0	0.0	0.0
4	HALLMARK_COAGULATION	123	-0.6698	-1.8226	0.0	2.563E-4	0.001
5	HALLMARK_KRAS_SIGNALING_UP	192	-0.6006	-1.7262	0.0	0.002215	0.01
6	HALLMARK_UV_RESPONSE_UP	156	-0.4506	-1.2664	0.09465	0.1691	0.963
7	HALLMARK_APOPTOSIS	158	-0.6032	-1.7071	0.0	0.002041	0.013
8	HALLMARK_ANGIOGENESIS	35	-0.7170	-1.6595	0.001684	0.004941	0.035
9	HALLMARK_IL6_JAK_STAT3_SIGNALING	85	-0.6260	-1.6475	0.0	0.005532	0.044
10	HALLMARK_IL2_STAT5_SIGNALING	199	-0.5697	-1.6413	0.0	0.005443	0.048
Positive enrichment in panitumumab-treated tissue							
1	HALLMARK_E2F_TARGETS	200	0.6800	2.2360	0.0	0.0	0.0

2	HALLMARK_G2M_CHECKPOINT	197	0.5627	1.8624	0.0	7.552E-4	0.002
3	HALLMARK_OXIDATIVE_PHOSPHORYLATION	200	0.5037	1.6815	0.0	0.003397	0.016
4	HALLMARK_KRAS_SIGNALING_DN	170	0.4213	1.3726	0.008658	0.06778	0.341
5	HALLMARK_INTERFERON_ALPHA_RESPONSE	96	0.4478	1.3532	0.03448	0.06472	0.39

ES, enrichment score; FDR, false discovery rate; FWER, familywise error rate; NES, normalized enrichment score.

Table S2. Differentially expressed genes in SUM149 tumor-infiltrating CD8$^+$ T cells after panitumumab treatment.

Gene Symbol	Encoded Protein	Log$_2$FC	Padj	Function
KLRC2	NKG2C	-3.174	0.000107	Is associated with NK cell functions (*78-81*).
CSF1	CSF1	-2.590	9.36E-05	Promotes the infiltration of TAMs and suppresses the effect of T cell functions (*33*).
S100A7	S100A7	-2.348	1.58E-05	Contributes to the formation of a pro-inflammatory environment that favors tumor progression and metastasis (*34*).
KLRC1	NKG2A	-2.177	5.13E-8	Blockade of KLRC1 on CD8$^+$ T cells can promote anti-tumor immunity by unleashing both T and NK cells (*32*).
S100A8	S100A8	-2.112	0.0057	Induces immunosuppressive TAMs and MDSC accumulation (*35, 82*).
*HAVCR2 (*also called *TIM3)*	HAVCR2 (TIM3)	-1.923	7.09E-05	Immune checkpoint (*83, 84*).
APOE	APOE	2.208	0.00061	Elicits anti-tumor responses and enhances T cell activation (*36*).
DUSP2	DUSP2	1.413	2.35E-05	Restrains T cell expansion and effector function; suppresses the host immune response against cancer (*85*).

LMNA	Lamin A/C	1.132	0.0161	Augments Th1 differentiation and response (*38, 86*).
ISG15	ISG15	1.297	0.000301	Enhances IFN-γ secretion by NK and T cells; promotes cytotoxic T lymphocyte response via NK cells (*37, 87, 88*).

IFN-γ, interferon gamma; NK, natural killer; TAM, tumor-associated macrophage.

Table S3. Patient characteristics (n = 8).

Characteristic	All Patients	Patients with pCR	Patients with Non-pCR
Age, years			
Median	57	57	57
Range	29-68	29-61	40-68
Race/ethnicity, no. (%)			
White	7 (88)	3	4
African American	1 (12)	0	1
Sex, no. (%)			
Female	8 (100)	3	5
Age, years, no. (%)			
< 50	2 (25)	1	1
$\geq$ 50	6 (75)	2	4
Menopausal status, no. (%)			
Premenopausal	3 (38)	1	2
Postmenopausal	5 (62)	2	3
Clinical N category, no. (%)			
N1	4 (50)	2	2
N2	0	0	0
N3	4 (50)	1	3
TNM stage at presentation, no. (%)			
III	8 (100)	3	5
IV	0	0	0
Nuclear grade, no. (%)			
2	3 (38)	0	3
3	5 (62)	3	2
Primary tumor subtype, no. (%)			
HR+HER2-	4 (50)	1	3
HR-HER2-	4 (50)	2	2

+, positive; -, negative; HR, hormone receptor; pCR, pathological complete response.

Table S4. Cytokines/chemokines affected by panitumumab treatment in SUM149-hu-NSG-SGM3 mice as identified with a cytokine antibody array.

Cytokine/Chemokine	Intensity in IgG2-Treated Tumor	Intensity in Panitumumab-Treated Tumor	Fold Change*
IP-10 (CXCL10)	3.725	33.214	8.92
RANTES (CCL5)	2.531	19.583	7.74
MIP-1b (CCL4)	4.092	11.217	2.74
MIG (CXCL9)	2.493	3.860	1.55
IL-8	27.622	16.620	0.60
GRO	43.592	25.288	0.58
Fractalkine (CX3CL1)	2.531	1.440	0.57
Osteoprotegerin (OPG)	8.053	1.877	0.23
MCP-1 (CCL2)	2.886	0.508	0.18
ENA-78 (CXCL5)	11.581	0.884	0.08
MIP-3α (CCL20)	7.804	0.194	0.02

* Fold change = intensity in panitumumab-treated tumor/intensity in IgG2-treated tumor.

REFERENCES AND NOTES

1. P. Schmid, J. Cortes, L. Pusztai, H. McArthur, S. Kummel, J. Bergh, C. Denkert, Y. H. Park, R. Hui, N. Harbeck, M. Takahashi, T. Foukakis, P. A. Fasching, F. Cardoso, M. Untch, L. Jia, V. Karantza, J. Zhao, G. Aktan, R. Dent, J. O'Shaughnessy; KEYNOTE-522 Investigators, Pembrolizumab for early triple-negative breast cancer. *N. Engl. J. Med.* **382**, 810–821 (2020).

2. E. A. Mittendorf, H. Zhang, C. H. Barrios, S. Saji, K. H. Jung, R. Hegg, A. Koehler, J. Sohn, H. Iwata, M. L. Telli, C. Ferrario, K. Punie, F. Penault-Llorca, S. Patel, A. N. Duc, M. Liste-Hermoso, V. Maiya, L. Molinero, S. Y. Chui, N. Harbeck, Neoadjuvant atezolizumab in combination with sequential nab-paclitaxel and anthracycline-based chemotherapy versus placebo and chemotherapy in patients with early-stage triple-negative breast cancer (IMpassion031): A randomised, double-blind, phase 3 trial. *Lancet* **396**, 1090–1100 (2020).

3. L. Gandhi, D. Rodriguez-Abreu, S. Gadgeel, E. Esteban, E. Felip, F. De Angelis, M. Domine, P. Clingan, M. J. Hochmair, S. F. Powell, S. Y. Cheng, H. G. Bischoff, N. Peled, F. Grossi, R. R. Jennens, M. Reck, R. Hui, E. B. Garon, M. Boyer, B. Rubio-Viqueira, S. Novello, T. Kurata, J. E. Gray, J. Vida, Z. Wei, J. Yang, H. Raftopoulos, M. C. Pietanza, M. C. Garassino; KEYNOTE-189 Investigators, Pembrolizumab plus chemotherapy in metastatic non-small-cell lung cancer. *N. Engl. J. Med.* **378**, 2078–2092 (2018).

4. L. Paz-Ares, A. Luft, D. Vicente, A. Tafreshi, M. Gumus, J. Mazieres, B. Hermes, F. Cay Senler, T. Csoszi, A. Fulop, J. Rodriguez-Cid, J. Wilson, S. Sugawara, T. Kato, K. H. Lee, Y. Cheng, S. Novello, B. Halmos, X. Li, G. M. Lubiniecki, B. Piperdi, D. M. Kowalski; KEYNOTE-407 Investigators, Pembrolizumab plus chemotherapy for squamous non-small-cell lung cancer. *N. Engl. J. Med.* **379**, 2040–2051 (2018).

5. C. Robert, G. V. Long, B. Brady, C. Dutriaux, M. Maio, L. Mortier, J. C. Hassel, P. Rutkowski, C. McNeil, E. Kalinka-Warzocha, K. J. Savage, M. M. Hernberg, C. Lebbe, J. Charles, C. Mihalcioiu, V. Chiarion-Sileni, C. Mauch, F. Cognetti, A. Arance, H. Schmidt, D. Schadendorf, H. Gogas, L. Lundgren-Eriksson, C. Horak, B. Sharkey, I. M. Waxman, V.

Atkinson, P. A. Ascierto, Nivolumab in previously untreated melanoma without BRAF mutation. *N. Engl. J. Med.* **372**, 320–330 (2015).

6. C. Robert, L. Thomas, I. Bondarenko, S. O'Day, J. Weber, C. Garbe, C. Lebbe, J. F. Baurain, A. Testori, J. J. Grob, N. Davidson, J. Richards, M. Maio, A. Hauschild, W. H. Miller, Jr., P. Gascon, M. Lotem, K. Harmankaya, R. Ibrahim, S. Francis, T. T. Chen, R. Humphrey, A. Hoos, J. D. Wolchok, Ipilimumab plus dacarbazine for previously untreated metastatic melanoma. *N. Engl. J. Med.* **364**, 2517–2526 (2011).

7. J. S. Weber, S. P. D'Angelo, D. Minor, F. S. Hodi, R. Gutzmer, B. Neyns, C. Hoeller, N. I. Khushalani, W. H. Miller Jr., C. D. Lao, G. P. Linette, L. Thomas, P. Lorigan, K. F. Grossmann, J. C. Hassel, M. Maio, M. Sznol, P. A. Ascierto, P. Mohr, B. Chmielowski, A. Bryce, I. M. Svane, J. J. Grob, A. M. Krackhardt, C. Horak, A. Lambert, A. S. Yang, J. Larkin, Nivolumab versus chemotherapy in patients with advanced melanoma who progressed after anti-CTLA-4 treatment (CheckMate 037): A randomised, controlled, open-label, phase 3 trial. *Lancet Oncol.* **16**, 375–384 (2015).

8. V. Anagnostou, K. N. Smith, P. M. Forde, N. Niknafs, R. Bhattacharya, J. White, T. Zhang, V. Adleff, J. Phallen, N. Wali, C. Hruban, V. B. Guthrie, K. Rodgers, J. Naidoo, H. Kang, W. Sharfman, C. Georgiades, F. Verde, P. Illei, Q. K. Li, E. Gabrielson, M. V. Brock, C. A. Zahnow, S. B. Baylin, R. B. Scharpf, J. R. Brahmer, R. Karchin, D. M. Pardoll, V. E. Velculescu, Evolution of neoantigen landscape during immune checkpoint blockade in non-small cell lung cancer. *Cancer Discov.* **7**, 264–276 (2017).

9. S. N. Gettinger, L. Horn, L. Gandhi, D. R. Spigel, S. J. Antonia, N. A. Rizvi, J. D. Powderly, R. S. Heist, R. D. Carvajal, D. M. Jackman, L. V. Sequist, D. C. Smith, P. Leming, D. P. Carbone, M. C. Pinder-Schenck, S. L. Topalian, F. S. Hodi, J. A. Sosman, M. Sznol, D. F. McDermott, D. M. Pardoll, V. Sankar, C. M. Ahlers, M. Salvati, J. M. Wigginton, M. D. Hellmann, G. D. Kollia, A. K. Gupta, J. R. Brahmer, Overall survival and long-term safety of nivolumab (anti-programmed death 1 antibody, BMS-936558, ONO-4538) in patients with previously treated advanced non-small-cell lung cancer. *J. Clin. Oncol.* **33**, 2004–2012 (2015).

10. C. M. Fares, E. M. Van Allen, C. G. Drake, J. P. Allison, S. Hu-Lieskovan, Mechanisms of resistance to immune checkpoint blockade: Why does checkpoint inhibitor immunotherapy not work for all patients? *Am. Soc. Clin. Oncol. Educ. Book* **39**, 147–164 (2019).

11. S. L. Highfill, Y. Cui, A. J. Giles, J. P. Smith, H. Zhang, E. Morse, R. N. Kaplan, C. L. Mackall, Disruption of CXCR2-mediated MDSC tumor trafficking enhances anti-PD1 efficacy. *Sci. Transl. Med.* **6**, 237ra267 (2014).

12. B. Ruffell, L. M. Coussens, Macrophages and therapeutic resistance in cancer. *Cancer Cell* **27**, 462–472 (2015).

13. A. Ribas, D. Lawrence, V. Atkinson, S. Agarwal, W. H. Miller Jr., M. S. Carlino, R. Fisher, G. V. Long, F. S. Hodi, J. Tsoi, C. S. Grasso, B. Mookerjee, Q. Zhao, R. Ghori, B. H. Moreno, N. Ibrahim, O. Hamid, Combined BRAF and MEK inhibition with PD-1 blockade immunotherapy in BRAF-mutant melanoma. *Nat. Med.* **25**, 936–940 (2019).

14. R. J. Sullivan, O. Hamid, R. Gonzalez, J. R. Infante, M. R. Patel, F. S. Hodi, K. D. Lewis, H. A. Tawbi, G. Hernandez, M. J. Wongchenko, Y. Chang, L. Roberts, M. Ballinger, Y. Yan, E. Cha, P. Hwu, Atezolizumab plus cobimetinib and vemurafenib in BRAF-mutated melanoma patients. *Nat. Med.* **25**, 929–935 (2019).

15. M. Cristofanilli, A. U. Buzdar, G. N. Hortobagyi, Update on the management of inflammatory breast cancer. *Oncologist* **8**, 141–148 (2003).

16. S. Dawood, N. T. Ueno, V. Valero, W. A. Woodward, T. A. Buchholz, G. N. Hortobagyi, A. M. Gonzalez-Angulo, M. Cristofanilli, Differences in survival among women with stage III inflammatory and noninflammatory locally advanced breast cancer appear early: A large population-based study. *Cancer* **117**, 1819–1826 (2011).

17. K. W. Hance, W. F. Anderson, S. S. Devesa, H. A. Young, P. H. Levine, Trends in inflammatory breast carcinoma incidence and survival: The surveillance, epidemiology, and end results program at the National Cancer Institute. *J. Natl. Cancer Inst.* **97**, 966–975 (2005).

18. H. Yamauchi, W. A. Woodward, V. Valero, R. H. Alvarez, A. Lucci, T. A. Buchholz, T. Iwamoto, S. Krishnamurthy, W. Yang, J. M. Reuben, G. N. Hortobagyi, N. T. Ueno, Inflammatory breast cancer: What we know and what we need to learn. *Oncologist* **17**, 891–899 (2012).

19. S. G. Allen, Y. C. Chen, J. M. Madden, C. L. Fournier, M. A. Altemus, A. B. Hiziroglu, Y. H. Cheng, Z. F. Wu, L. Bao, J. A. Yates, E. Yoon, S. D. Merajver, Macrophages enhance migration in inflammatory breast cancer cells via RhoC GTPase signaling. *Sci. Rep.* **6**, 39190 (2016).

20. L. Lacerda, B. G. Debeb, D. Smith, R. Larson, T. Solley, W. Xu, S. Krishnamurthy, Y. Gong, L. B. Levy, T. Buchholz, N. T. Ueno, A. Klopp, W. A. Woodward, Mesenchymal stem cells mediate the clinical phenotype of inflammatory breast cancer in a preclinical model. *Breast Cancer Res.* **17**, 42 (2015).

21. A. R. Wolfe, N. J. Trenton, B. G. Debeb, R. Larson, B. Ruffell, K. Chu, W. Hittelman, M. Diehl, J. M. Reuben, N. T. Ueno, W. A. Woodward, Mesenchymal stem cells and macrophages interact through IL-6 to promote inflammatory breast cancer in pre-clinical models. *Oncotarget* **7**, 82482–82492 (2016).

22. F. Bertucci, N. T. Ueno, P. Finetti, P. Vermeulen, A. Lucci, F. M. Robertson, M. Marsan, T. Iwamoto, S. Krishnamurthy, H. Masuda, P. Van Dam, W. A. Woodward, M. Cristofanilli, J. M. Reuben, L. Dirix, P. Viens, W. F. Symmans, D. Birnbaum, S. J. Van Laere, Gene expression profiles of inflammatory breast cancer: Correlation with response to neoadjuvant chemotherapy and metastasis-free survival. *Ann. Oncol.* **25**, 358–365 (2014).

23. S. M. Reddy, A. Reuben, S. Barua, H. Jiang, S. Zhang, L. Wang, V. Gopalakrishnan, C. W. Hudgens, M. T. Tetzlaff, J. M. Reuben, T. Tsujikawa, L. M. Coussens, K. Wani, Y. He, L. Villareal, A. Wood, A. Rao, W. A. Woodward, N. T. Ueno, S. Krishnamurthy, J. A. Wargo, E. A. Mittendorf, Poor response to neoadjuvant chemotherapy correlates with mast cell infiltration in inflammatory breast cancer. *Cancer Immunol. Res.* **7**, 1025–1035 (2019).

24. N. Cabioglu, Y. Gong, R. Islam, K. R. Broglio, N. Sneige, A. Sahin, A. M. Gonzalez-Angulo, P. Morandi, C. Bucana, G. N. Hortobagyi, M. Cristofanilli, Expression of growth factor and chemokine receptors: New insights in the biology of inflammatory breast cancer. *Ann. Oncol.* **18**, 1021–1029 (2007).

25. B. Corkery, J. Crown, M. Clynes, N. O'Donovan, Epidermal growth factor receptor as a potential therapeutic target in triple-negative breast cancer. *Ann. Oncol.* **20**, 862–867 (2009).

26. N. Matsuda, X. Wang, B. Lim, S. Krishnamurthy, R. H. Alvarez, J. S. Willey, C. A. Parker, J. Song, Y. Shen, J. Hu, W. Wu, N. Li, G. V. Babiera, J. L. Murray, B. K. Arun, A. M. Brewster, J. M. Reuben, M. C. Stauder, C. M. Barnett, W. A. Woodward, H. T. C. Le-Petross, A. Lucci, S. M. DeSnyder, D. Tripathy, V. Valero, N. T. Ueno, Safety and efficacy of panitumumab plus neoadjuvant chemotherapy in patients with primary HER2-negative inflammatory breast cancer. *JAMA Oncol.* **4**, 1207–1213 (2018).

27. F. Ishikawa, M. Yasukawa, B. Lyons, S. Yoshida, T. Miyamoto, G. Yoshimoto, T. Watanabe, K. Akashi, L. D. Shultz, M. Harada, Development of functional human blood and immune systems in NOD/SCID/IL2 receptor γ chainnull mice. *Blood* **106**, 1565–1573 (2005).

28. L. D. Shultz, M. A. Brehm, J. V. Garcia-Martinez, D. L. Greiner, Humanized mice for immune system investigation: Progress, promise and challenges. *Nat. Rev. Immunol.* **12**, 786–798 (2012).

29. J. P. Huber, J. D. Farrar, Regulation of effector and memory T-cell functions by type I interferon. *Immunology* **132**, 466–474 (2011).

30. A. Le Bon, D. F. Tough, Links between innate and adaptive immunity via type I interferon. *Curr. Opin. Immunol.* **14**, 432–436 (2002).

31. B. S. Parker, J. Rautela, P. J. Hertzog, Antitumour actions of interferons: Implications for cancer therapy. *Nat. Rev. Cancer* **16**, 131–144 (2016).

32. P. Andre, C. Denis, C. Soulas, C. Bourbon-Caillet, J. Lopez, T. Arnoux, M. Blery, C. Bonnafous, L. Gauthier, A. Morel, B. Rossi, R. Remark, V. Breso, E. Bonnet, G. Habif, S. Guia, A. I. Lalanne, C. Hoffmann, O. Lantz, J. Fayette, A. Boyer-Chammard, R. Zerbib, P. Dodion, H. Ghadially, M. Jure-Kunkel, Y. Morel, R. Herbst, E. Narni-Mancinelli, R. B. Cohen, E. Vivier, Anti-NKG2A mAb is a checkpoint inhibitor that promotes anti-tumor immunity by unleashing both T and NK cells. *Cell* **175**, 1731–1743.e13 (2018).

33. Y. Zhu, B. L. Knolhoff, M. A. Meyer, T. M. Nywening, B. L. West, J. Luo, A. Wang-Gillam, S. P. Goedegebuure, D. C. Linehan, D. G. DeNardo, CSF1/CSF1R blockade reprograms tumor-infiltrating macrophages and improves response to T-cell checkpoint immunotherapy in pancreatic cancer models. *Cancer Res.* **74**, 5057–5069 (2014).

34. L. Padilla, S. Dakhel, J. Adan, M. Masa, J. M. Martinez, L. Roque, T. Coll, R. Hervas, C. Calvis, L. Llinas, S. Buenestado, J. Castellsague, R. Messeguer, F. Mitjans, J. L. Hernandez, S100A7: From mechanism to cancer therapy. *Oncogene* **36**, 6749–6761 (2017).

35. P. Sinha, C. Okoro, D. Foell, H. H. Freeze, S. Ostrand-Rosenberg, G. Srikrishna, Proinflammatory S100 proteins regulate the accumulation of myeloid-derived suppressor cells. *J. Immunol.* **181**, 4666–4675 (2008).

36. M. F. Tavazoie, I. Pollack, R. Tanqueco, B. N. Ostendorf, B. S. Reis, F. C. Gonsalves, I. Kurth, C. Andreu-Agullo, M. L. Derbyshire, J. Posada, S. Takeda, K. N. Tafreshian, E. Rowinsky, M. Szarek, R. J. Waltzman, E. A. McMillan, C. Zhao, M. Mita, A. Mita, B. Chmielowski, M. A. Postow, A. Ribas, D. Mucida, S. F. Tavazoie, LXR/apoe activation restricts innate immune suppression in cancer. *Cell* **172**, 825–840.e18 (2018).

37. J. D'Cunha, E. Knight, Jr., A. L. Haas, R. L. Truitt, E. C. Borden, Immunoregulatory properties of ISG15, an interferon-induced cytokine. *Proc. Natl. Acad. Sci. U.S.A.* **93**, 211–215 (1996).

38. V. Rocha-Perugini, J. M. Gonzalez-Granado, Nuclear envelope lamin-A as a coordinator of T cell activation. *Nucleus* **5**, 396–401 (2014).

39. A. L. Chang, J. Miska, D. A. Wainwright, M. Dey, C. V. Rivetta, D. Yu, D. Kanojia, K. C. Pituch, J. Qiao, P. Pytel, Y. Han, M. Wu, L. Zhang, C. M. Horbinski, A. U. Ahmed, M. S. Lesniak, CCL2 produced by the glioma microenvironment is essential for the recruitment of regulatory T cells and myeloid-derived suppressor cells. *Cancer Res.* **76**, 5671–5682 (2016).

40. K. W. Cook, D. P. Letley, R. J. Ingram, E. Staples, H. Skjoldmose, J. C. Atherton, K. Robinson, CCL20/CCR6-mediated migration of regulatory T cells to the *Helicobacter pylori*-infected human gastric mucosa. *Gut* **63**, 1550–1559 (2014).

41. Z. G. Fridlender, J. Sun, I. Mishalian, S. Singhal, G. Cheng, V. Kapoor, W. Horng, G. Fridlender, R. Bayuh, G. S. Worthen, S. M. Albelda, Transcriptomic analysis comparing tumor-associated neutrophils with granulocytic myeloid-derived suppressor cells and normal neutrophils. *PLOS ONE* **7**, e31524 (2012).

42. J. Mei, Y. Liu, N. Dai, M. Favara, T. Greene, S. Jeyaseelan, M. Poncz, J. S. Lee, G. S. Worthen, CXCL5 regulates chemokine scavenging and pulmonary host defense to bacterial infection. *Immunity* **33**, 106–117 (2010).

43. K. O. Osuala, B. F. Sloane, Many roles of CCL20: Emphasis on breast cancer. *Postdoc. J.* **2**, 7–16 (2014).

44. D. Dangaj, M. Bruand, A. J. Grimm, C. Ronet, D. Barras, P. A. Duttagupta, E. Lanitis, J. Duraiswamy, J. L. Tanyi, F. Benencia, J. Conejo-Garcia, H. R. Ramay, K. T. Montone, D. J. Powell Jr., P. A. Gimotty, A. Facciabene, D. G. Jackson, J. S. Weber, S. J. Rodig, S. F. Hodi, L. E. Kandalaft, M. Irving, L. Zhang, P. Foukas, S. Rusakiewicz, M. Delorenzi, G. Coukos, Cooperation between constitutive and inducible chemokines enables T cell engraftment and immune attack in solid tumors. *Cancer Cell* **35**, 885–900.e10 (2019).

45. H. Harlin, Y. Meng, A. C. Peterson, Y. Zha, M. Tretiakova, C. Slingluff, M. McKee, T. F. Gajewski, Chemokine expression in melanoma metastases associated with CD8^{+} T-cell recruitment. *Cancer Res.* **69**, 3077–3085 (2009).

46. I. Bieche, F. Lerebours, S. Tozlu, M. Espie, M. Marty, R. Lidereau, Molecular profiling of inflammatory breast cancer: Identification of a poor-prognosis gene expression signature. *Clin. Cancer Res.* **10**, 6789–6795 (2004).

47. M. Gururajan, A. Simmons, T. Dasu, B. T. Spear, C. Calulot, D. A. Robertson, D. L. Wiest, J. G. Monroe, S. Bondada, Early growth response genes regulate B cell development, proliferation, and immune response. *J. Immunol.* **181**, 4590–4602 (2008).

48. S. B. McMahon, J. G. Monroe, The role of early growth response gene 1 (egr-1) in regulation of the immune response. *J. Leukoc. Biol.* **60**, 159–166 (1996).

49. H. Masuda, T. M. Brewer, D. D. Liu, T. Iwamoto, Y. Shen, L. Hsu, J. S. Willey, A. M. Gonzalez-Angulo, M. Chavez-MacGregor, T. M. Fouad, W. A. Woodward, J. M. Reuben, V. Valero, R. H. Alvarez, G. N. Hortobagyi, N. T. Ueno, Long-term treatment efficacy in primary inflammatory breast cancer by hormonal receptor- and HER2-defined subtypes. *Ann. Oncol.* **25**, 384–391 (2014).

50. A. M. Lesokhin, T. M. Hohl, S. Kitano, C. Cortez, D. Hirschhorn-Cymerman, F. Avogadri, G. A. Rizzuto, J. J. Lazarus, E. G. Pamer, A. N. Houghton, T. Merghoub, J. D. Wolchok, Monocytic CCR2$^+$ myeloid-derived suppressor cells promote immune escape by limiting activated CD8 T-cell infiltration into the tumor microenvironment. *Cancer Res.* **72**, 876–886 (2012).

51. J. P. Bottcher, E. Bonavita, P. Chakravarty, H. Blees, M. Cabeza-Cabrerizo, S. Sammicheli, N. C. Rogers, E. Sahai, S. Zelenay, E. S. C. Reis, NK cells stimulate recruitment of cDC1 into the tumor microenvironment promoting cancer immune control. *Cell* **172**, 1022–1037.e14 (2018).

52. E. Sugiyama, Y. Togashi, Y. Takeuchi, S. Shinya, Y. Tada, K. Kataoka, K. Tane, E. Sato, G. Ishii, K. Goto, Y. Shintani, M. Okumura, M. Tsuboi, H. Nishikawa, Blockade of EGFR improves responsiveness to PD-1 blockade in EGFR-mutated non-small cell lung cancer. *Sci. Immunol.* **5**, eaav3937 (2020).

53. L. D. Shultz, Y. Saito, Y. Najima, S. Tanaka, T. Ochi, M. Tomizawa, T. Doi, A. Sone, N. Suzuki, H. Fujiwara, M. Yasukawa, F. Ishikawa, Generation of functional human T-cell subsets with HLA-restricted immune responses in HLA class I expressing NOD/SCID/IL2r gamma(null) humanized mice. *Proc. Natl. Acad. Sci. U.S.A.* **107**, 13022–13027 (2010).

54. M. Van den Eynde, B. Mlecnik, G. Bindea, T. Fredriksen, S. E. Church, L. Lafontaine, N. Haicheur, F. Marliot, M. Angelova, A. Vasaturo, D. Bruni, A. Jouret-Mourin, P. Baldin, N. Huyghe, K. Haustermans, A. Debucquoy, E. Van Cutsem, J. F. Gigot, C. Hubert, A. Kartheuser, C. Remue, D. Leonard, V. Valge-Archer, F. Pages, J. P. Machiels, J. Galon, The link between the multiverse of immune microenvironments in metastases and the survival of colorectal cancer patients. *Cancer Cell* **34**, 1012–1026.e3 (2018).

55. T. Liang, W. Tong, S. Ma, P. Chang, Standard therapies: Solutions for improving therapeutic effects of immune checkpoint inhibitors on colorectal cancer. *Onco. Targets. Ther.* **9**, 1773205 (2020).

56. L. Li, A. H. Ameri, S. Wang, K. H. Jansson, O. M. Casey, Q. Yang, M. L. Beshiri, L. Fang, R. G. Lake, S. Agarwal, A. N. Alilin, W. Xu, J. Yin, K. Kelly, EGR1 regulates angiogenic and osteoclastogenic factors in prostate cancer and promotes metastasis. *Oncogene* **38**, 6241–6255 (2019).

57. Z. Ma, X. Gao, Y. Shuai, X. Wu, Y. Yan, X. Xing, J. Ji, EGR1-mediated linc01503 promotes cell cycle progression and tumorigenesis in gastric cancer. *Cell Prolif.* **54**, e12922 (2021).

58. T. Mohamad, N. Kazim, A. Adhikari, J. K. Davie, EGR1 interacts with TBX2 and functions as a tumor suppressor in rhabdomyosarcoma. *Oncotarget* **9**, 18084–18098 (2018).

59. L. Su, H. Cheng, A. V. Sampaio, T. O. Nielsen, T. M. Underhill, EGR1 reactivation by histone deacetylase inhibitors promotes synovial sarcoma cell death through the PTEN tumor suppressor. *Oncogene* **29**, 4352–4361 (2010).

60. T. Stuart, A. Butler, P. Hoffman, C. Hafemeister, E. Papalexi, W. M. Mauck III, Y. Hao, M. Stoeckius, P. Smibert, R. Satija, Comprehensive integration of single-cell data. *Cell* **177**, 1888–1902.e21 (2019).

61. E. Becht, L. McInnes, J. Healy, C. A. Dutertre, I. W. H. Kwok, L. G. Ng, F. Ginhoux, E. W. Newell, Dimensionality reduction for visualizing single-cell data using UMAP. *Nat. Biotechnol.* **37**, 38–44 (2019).

62. M. A. Al Barashdi, A. Ali, M. F. McMullin, K. Mills, Protein tyrosine phosphatase receptor type C (PTPRC or CD45). *J. Clin. Pathol.* **74**, 548–552 (2021).

63. C. Chen, D. Nadal, S. A. Cohen, E. Schläpfer, B. K. Mookerjee, A. Vladutiu, M. W. Stinson, P. L. Ogra, B. Albini, Direct demonstration of engraftment of human peripheral blood leukocytes in SCID mice. *Int. Arch. Allergy Immunol.* **97**, 295–300 (1992).

64. F. O. Martinez, S. Gordon, The M1 and M2 paradigm of macrophage activation: Time for reassessment. *F1000Prime Rep* **6**, 13 (2014).

65. I. Tirosh, B. Izar, S. M. Prakadan, M. H. Wadsworth II, D. Treacy, J. J. Trombetta, A. Rotem, C. Rodman, C. Lian, G. Murphy, M. Fallahi-Sichani, K. Dutton-Regester, J. R. Lin, O. Cohen, P. Shah, D. Lu, A. S. Genshaft, T. K. Hughes, C. G. Ziegler, S. W. Kazer, A. Gaillard, K. E. Kolb, A. C. Villani, C. M. Johannessen, A. Y. Andreev, E. M. Van Allen, M. Bertagnolli, P. K. Sorger, R. J. Sullivan, K. T. Flaherty, D. T. Frederick, J. Jane-Valbuena, C. H. Yoon, O. Rozenblatt-Rosen, A. K. Shalek, A. Regev, L. A. Garraway, Dissecting the multicellular ecosystem of metastatic melanoma by single-cell RNA-seq. *Science* **352**, 189–196 (2016).

66. S. T. Trifonova, J. Zimmer, J. D. Turner, C. P. Muller, Diurnal redistribution of human lymphocytes and their temporal associations with salivary cortisol. *Chronobiol. Int.* **30**, 669–681 (2013).

67. M. I. Love, W. Huber, S. Anders, Moderated estimation of fold change and dispersion for RNA-seq data with DESeq2. *Genome Biol.* **15**, 550 (2014).

68. A. Liberzon, C. Birger, H. Thorvaldsdottir, M. Ghandi, J. P. Mesirov, P. Tamayo, The Molecular Signatures Database (MSigDB) hallmark gene set collection. *Cell Syst.* **1**, 417–425 (2015).

69. X. Wang, M. E. Reyes, D. Zhang, Y. Funakoshi, A. P. Trape, Y. Gong, T. Kogawa, B. L. Eckhardt, H. Masuda, D. A. Pirman Jr., P. Yang, J. M. Reuben, W. A. Woodward, C. Bartholomeusz, G. N. Hortobagyi, D. Tripathy, N. T. Ueno, EGFR signaling promotes inflammation and cancer stem-like activity in inflammatory breast cancer. *Oncotarget* **8**, 67904–67917 (2017).

70. S. J. Van Laere, N. T. Ueno, P. Finetti, P. Vermeulen, A. Lucci, F. M. Robertson, M. Marsan, T. Iwamoto, S. Krishnamurthy, H. Masuda, P. van Dam, W. A. Woodward, P. Viens, M. Cristofanilli, D. Birnbaum, L. Dirix, J. M. Reuben, F. Bertucci, Uncovering the molecular secrets of inflammatory breast cancer biology: An integrated analysis of three distinct affymetrix gene expression datasets. *Clin. Cancer Res.* **19**, 4685–4696 (2013).

71. S. Dawood, S. D. Merajver, P. Viens, P. B. Vermeulen, S. M. Swain, T. A. Buchholz, L. Y. Dirix, P. H. Levine, A. Lucci, S. Krishnamurthy, F. M. Robertson, W. A. Woodward, W. T. Yang, N. T. Ueno, M. Cristofanilli, International expert panel on inflammatory breast cancer: Consensus statement for standardized diagnosis and treatment. *Ann. Oncol.* **22**, 515–523 (2011).

72. R. A. Irizarry, B. Hobbs, F. Collin, Y. D. Beazer-Barclay, K. J. Antonellis, U. Scherf, T. P. Speed, Exploration, normalization, and summaries of high density oligonucleotide array probe level data. *Biostatistics* **4**, 249–264 (2003).

73. W. E. Johnson, C. Li, A. Rabinovic, Adjusting batch effects in microarray expression data using empirical Bayes methods. *Biostatistics* **8**, 118–127 (2007).

74. J. Taminau, D. Steenhoff, A. Coletta, S. Meganck, C. Lazar, V. de Schaetzen, R. Duque, C. Molter, H. Bersini, A. Nowé, D. Y. W. Solís, inSilicoDb: An R/Bioconductor package for accessing human Affymetrix expert-curated datasets from GEO. *Bioinformatics* **27**, 3204–3205 (2011).

75. B. D. Lehmann, J. A. Bauer, X. Chen, M. E. Sanders, A. B. Chakravarthy, Y. Shyr, J. A. Pietenpol, Identification of human triple-negative breast cancer subtypes and preclinical models for selection of targeted therapies. *J. Clin. Invest.* **121**, 2750–2767 (2011).

76. I. Sicking, K. Rommens, M. J. Battista, D. Bohm, S. Gebhard, A. Lebrecht, C. Cotarelo, G. Hoffmann, J. G. Hengstler, M. Schmidt, Prognostic influence of cyclooxygenase-2 protein and mRNA expression in node-negative breast cancer patients. *BMC Cancer* **14**, 952 (2014).

77. X. Wang, H. Saso, T. Iwamoto, W. Xia, Y. Gong, L. Pusztai, W. A. Woodward, J. M. Reuben, S. L. Warner, D. J. Bearss, G. N. Hortobagyi, M. C. Hung, N. T. Ueno, TIG1 promotes the development and progression of inflammatory breast cancer through activation of Axl kinase. *Cancer Res.* **73**, 6516–6525 (2013).

78. Y. Ding, S. Sumitran, J. Holgersson, Direct binding of purified HLA class I antigens by soluble NKG2/CD94 C-type lectins from natural killer cells. *Scand. J. Immunol.* **49**, 459–465 (1999).

79. V. M. Braud, D. S. Allan, C. A. O'Callaghan, K. Soderstrom, A. D'Andrea, G. S. Ogg, S. Lazetic, N. T. Young, J. I. Bell, J. H. Phillips, L. L. Lanier, A. J. McMichael, HLA-E binds to natural killer cell receptors CD94/NKG2A, B and C. *Nature* **391**, 795–799 (1998).

80. S. Lazetic, C. Chang, J. P. Houchins, L. L. Lanier, J. H. Phillips, Human natural killer cell receptors involved in MHC class I recognition are disulfide-linked heterodimers of CD94 and NKG2 subunits. *J. Immunol.* **157**, 4741–4745 (1996).

81. N. Lee, M. Llano, M. Carretero, A. Ishitani, F. Navarro, M. Lopez-Botet, D. E. Geraghty, HLA-E is a major ligand for the natural killer inhibitory receptor CD94/NKG2A. *Proc. Natl. Acad. Sci. U.S.A.* **95**, 5199–5204 (1998).

82. P. Cheng, C. A. Corzo, N. Luetteke, B. Yu, S. Nagaraj, M. M. Bui, M. Ortiz, W. Nacken, C. Sorg, T. Vogl, J. Roth, D. I. Gabrilovich, Inhibition of dendritic cell differentiation and accumulation of myeloid-derived suppressor cells in cancer is regulated by S100A9 protein. *J. Exp. Med.* **205**, 2235–2249 (2008).

83. S. D. Blackburn, H. Shin, W. N. Haining, T. Zou, C. J. Workman, A. Polley, M. R. Betts, G. J. Freeman, D. A. Vignali, E. J. Wherry, Coregulation of CD8^{+} T cell exhaustion by multiple inhibitory receptors during chronic viral infection. *Nat. Immunol.* **10**, 29–37 (2009).

84. L. Monney, C. A. Sabatos, J. L. Gaglia, A. Ryu, H. Waldner, T. Chernova, S. Manning, E. A. Greenfield, A. J. Coyle, R. A. Sobel, G. J. Freeman, V. K. Kuchroo, Th1-specific cell surface protein Tim-3 regulates macrophage activation and severity of an autoimmune disease. *Nature* **415**, 536–541 (2002).

85. L. Dan, L. Liu, Y. Sun, J. Song, Q. Yin, G. Zhang, F. Qi, Z. Hu, Z. Yang, Z. Zhou, Y. Hu, L. Zhang, J. Ji, X. Zhao, Y. Jin, M. A. McNutt, Y. Yin, The phosphatase PAC1 acts as a T cell suppressor and attenuates host antitumor immunity. *Nat. Immunol.* **21**, 287–297 (2020).

86. R. Toribio-Fernandez, V. Zorita, V. Rocha-Perugini, S. Iborra, G. Martinez Del Hoyo, R. Chevre, B. Dorado, D. Sancho, F. Sanchez-Madrid, V. Andres, J. M. Gonzalez-Granado, Lamin A/C augments Th1 differentiation and response against *Vaccinia virus* and *Leishmania major*. *Cell Death Dis.* **9**, 9 (2018).

87. D. Bogunovic, M. Byun, L. A. Durfee, A. Abhyankar, O. Sanal, D. Mansouri, S. Salem, I. Radovanovic, A. V. Grant, P. Adimi, N. Mansouri, S. Okada, V. L. Bryant, X. F. Kong, A. Kreins, M. M. Velez, B. Boisson, S. Khalilzadeh, U. Ozcelik, I. A. Darazam, J. W. Schoggins, C. M. Rice, S. Al-Muhsen, M. Behr, G. Vogt, A. Puel, J. Bustamante, P. Gros, J. M. Huibregtse, L. Abel, S. Boisson-Dupuis, J. L. Casanova, Mycobacterial disease and impaired IFN-γ immunity in humans with inherited ISG15 deficiency. *Science* **337**, 1684–1688 (2012).

88. V. Iglesias-Guimarais, T. Ahrends, E. de Vries, K. P. Knobeloch, A. Volkov, J. Borst, IFN-stimulated gene 15 is an alarmin that boosts the CTL response via an innate, NK cell-dependent route. *J. Immunol.* **204**, 2110–2121 (2020).